Synthesis of Nonspherical Microcapsules through Controlled Polyelectrolyte Coating of Hydrogel Templates

Langmuir

Article

pubs.acs.org/Langmuir

Synthesis of Nonspherical Microcapsules through Controlled Polyelectrolyte Coating of Hydrogel Templates

Lynna Chen,[†] Harry Z. An,[‡] and Patrick S. Doyle*[,‡]

[†]Department of Biological Engineering and [‡]Department of Chemical Engineering, Massachusetts Institute of Technology, Cambridge, Massachusetts 02139, United States

Supporting Information

ABSTRACT: We report a simple approach to fabricate custom-shape microcapsules using hydrogel templates synthesized by stop flow lithography. Cargo-containing microcapsules were made by coating hydrogel particles with a single layer of poly-L-lysine followed by a one-step core degradation and capsule cross-linking procedure. We determined appropriate coating conditions by investigating the effect of pH, ionic strength, and prepolymer composition on the diffusion of polyelectrolytes into the oppositely charged hydrogel template. We also characterized the degradation of the templating core by tracking the diffusivity of nanoparticles embedded within the hydrogel. Unlike any other technique, this approach allows for easy fabrication of microcapsules with internal features (e.g., toroids) and selective surface modification of Janus particles using any polyelectrolyte. These soft, flexible capsules may be useful for therapeutic applications as well as fundamental studies of membrane mechanics.

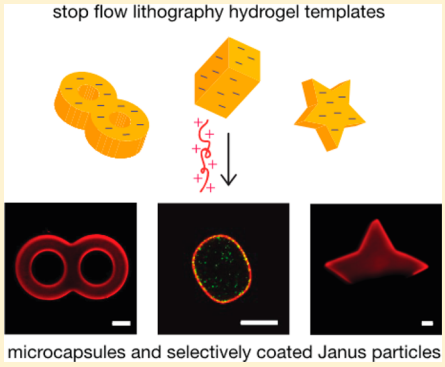

INTRODUCTION

Microparticles and microcapsules with customizable shape, mechanical flexibility, and surface anisotropy have received attention in recent years for their role in biomedical applications ranging from drug delivery to cell mimics for fundamental studies in flow.[1−5] Various techniques for the controlled synthesis of nonspherical microparticles have been developed,[6,7] including flow lithography,[8] nonwetting template molding (PRINT),[9] electrohydrodynamic jetting,[10] droplet microfluidics,[11] and film stretching.[12] However, solid microparticles are often inefficient at carrying cargo for therapeutic or diagnostic purposes. An ideal carrier would be a cargo-filled capsule with optimized shape and flexibility, as exemplified by the body's natural delivery vehicle—the red blood cell. However, synthetic microcapsules with these properties remain a challenge to fabricate due to limitations in template shape or material chemistry.

Several groups have fabricated nonspherical microcapsules by coating sacrificial templates using layer-by-layer techniques (LbL) and subsequently removing the core. Templates include solid polymer microparticles,[13−15] sacrificial biological entities such as red blood cells,[16,17] and microparticles made from inorganic materials—both porous (e.g., calcium carbonate,[18] manganese carbonate,[19] silica[4]) and nonporous (e.g., silicon[20]). Shortcomings of these templating strategies include restricted geometries and difficult loading of active therapeutics due to material incompatibility or processing conditions. Alternatively, spheroidal capsules have been made through arrested coalescence or mechanical squeezing of particle-decorated droplets.[21−25] For this approach, the range of shapes generated is very limited, resulting suspensions are often polydisperse, and capsule sizes are usually very large (i.e., 100−1000 μm).

Stop flow lithography (SFL), a technique that combines microfluidics with photolithography, can be used to fabricate hydrogel microparticles with any 2D-extruded shape in a high-throughput manner.[8,26] Previous work has shown that this technique can be used to create anisotropic striped particles with different chemical compositions[27] and entrap biologics and small molecule therapeutics in the biocompatible and easily functionalizable hydrogel matrix.[28,29] These properties make SFL microparticles attractive candidates for microcapsule templates.

In this work, we create custom-shape microcapsules using SFL particle templates, which can encapsulate nanoscale cargo. We coat microparticles (10−200 μm in size) using a single polyelectrolyte layer, creating core−shell structures with micron thick shells created by diffusion of the polyelectrolyte into the oppositely charged hydrogel matrix. We demonstrate how we can subsequently dissolve away particle cores, leaving behind mechanically flexible hollow capsules that retain complex template geometries. We show how to control the diffusion of the polyelectrolyte into the particle matrix, and hence the effective shell thickness, by tuning parameters including pH, ionic strength, and hydrogel prepolymer composition.

Our approach enables easy surface modification of nonspherical hydrogel particles that can be applied to a variety of polyelectrolytes, with the capability to selectively functionalize

Received: June 15, 2015
Revised: July 28, 2015

DOI: 10.1021/acs.langmuir.5b02200
Langmuir XXXX, XXX, XXX−XXX

Janus or patchy particles. With one additional step, we can fabricate hollow microcapsules in any lithographically defined shape. In contrast to the majority of capsules formed by LbL, our capsules only require deposition of a single polyelectrolyte layer, eliminating many time-consuming coating and rinsing steps. To our knowledge, this is the first demonstration of microcapsules fabricated using hydrogel templates with customizable shape and size.

EXPERIMENTAL SECTION

Materials. Poly(ethylene glycol) diacrylate (M_n = 700 g/mol), acrylic acid (anhydrous, ≥99.0%), poly(ethylene glycol) (M_n = 200 g/mol), 2-hydroxy-2-methyl-1-phenylpropan-1-one (Darocur 1173), poly-L-lysine hydrobromide (M_v = 150−300 kDa), hydrochloric acid (37%), *N*-(3-(dimethylamino)propyl)-*N*′-ethylcarbodiimide hydrochloride (≥99.0%), dimethyl sulfoxide (≥99.9%), and glycerol (≥99%) were purchased from Sigma-Aldrich and used as received. Fluorescein isothiocyanate dextran sulfate sodium (M_w = 46 000 g/mol) was purchased from TdB Consultancy. Fluoresbrite carboxy YG microspheres (2.6% solids in water, diameter = 0.19 ± 0.0092 μm, $\lambda_{ex}/\lambda_{em}$ = 441/486 nm) were purchased from Polysciences. Methacryloxyethyl thiocarbomoyl rhodamine B ($\lambda_{ex}/\lambda_{em}$ = 548/570 nm, Polysciences) and cyanine5 *N*-hydroxysuccinimide ($\lambda_{ex}/\lambda_{em}$ = 646/662 nm, Lumiprobe) were used for fluorescent labeling. PBST was made with 1X phosphate buffered saline (without calcium and magnesium, Corning) and 0.05% (v/v) Tween 20 (Sigma-Aldrich). Sodium chloride (crystal, Mallinckrodt Pharmaceuticals), sodium bicarbonate (powder, J.T. Baker), and sodium hydroxide (pellet, Macron Fine Chemicals) were dissolved in deionized water before use.

Particle Synthesis. All particles were fabricated via stop flow lithography as previously described,[8,26] using a prepolymer composition of 50% poly(ethylene glycol) diacrylate (PEGDA), 30% acrylic acid (AAc), 5% photoinitiator (Darocur 1173), and 15% deionized water, by volume, in rectangular PDMS (Sylgard 184, Dow Corning) microfluidic channels ranging from 30 to 55 μm in height. Fluorescently labeled particles were made by substituting 5% water with 5% 1 mg/mL rhodamine acrylate dissolved in poly(ethylene) glycol (PEG). Nanoparticle-containing prepolymer solution was made by substituting 3% water with 3% carboxylate polystyrene bead stock solution. Janus particles were synthesized using two-inlet devices with two different prepolymer solutions[8]—one as described above and the other containing 65% PEGDA, 30% PEG, and 5% photoinitiator.

Briefly, microfluidic devices were fabricated by curing PDMS (10:1 monomer to curing agent) on a silicon wafer patterned with SU-8 features and bonding devices onto a PDMS-coated glass slide. Prepolymer solution was loaded into the device using modified pipet tips, and an automated system was used to control the pressure-driven flow in the device. During each synthesis cycle, the solution flow was stopped, particles were polymerized by ultraviolet (UV) light (Lumen 200 metal arc lamp, Prior Scientific) through a UV filter set (11000v3-UV, Chroma Technology, 365 nm, 150 ms exposure time, 2200 mW/cm^2) in a mask defined shape (designed using AutoCAD, printed by Fineline Imaging), and the particles were collected in a microcentrifuge tube by resuming prepolymer flow. Particles were rinsed four times with PBST by centrifugation (300−2000 rcf for 10−30 s, depending on particle size) and stored in PBST at 4 °C.

Fluorescent Labeling of PLL. Poly-L-lysine (PLL) was covalently labeled with cyanine5 NHS ester by reacting dye with PLL in 10% dimethyl sulfoxide/90% (v/v) pH 8.5 solution of 0.1 M sodium bicarbonate at room temperature for 4 h on a horizontal shaker (350 rpm) to form an amide bond. The final solution concentrations of PLL and Cy5-NHS were 2 and 0.044 mg/mL, respectively. Unreacted dye was removed using a centrifugal filter unit (Amicon Ultra-4, Millipore). Labeled PLL was stored at a concentration of approximately 15 mg/mL in deionized water.

Polyelectrolyte Coating of Particles. Washed particles were added to a polyelectrolyte solution with defined ionic strength and pH in a microcentrifuge tube. Ionic strength was adjusted by varying the amount of NaCl dissolved in deionized water, and pH was adjusted by adding hydrochloric acid (HCl) or sodium hydroxide (NaOH). The pH was freshly adjusted each time the particles were coated. The final solution containing ∼5000 particles/mL and a polyelectrolyte concentration of 1 mg/mL was vortexed for 30 s and placed on a horizontal shaker (650 rpm) at room temperature for 5 min. Particles were rinsed four times with PBST by centrifugation (300−2000 rcf for 10−30 s, depending on particle size) and stored in PBST at 4 °C. The above steps were repeated to add oppositely charged polyelectrolyte layers.

Fabrication of Microcapsules. PLL-coated particles were transferred into small wells made from PDMS slabs with circular cutouts (4−8 mm in diameter), sandwiched between clean glass slides to prevent evaporation. The wells were filled with NaOH (final concentration: 10% (v/v) PBST (from particle solution), 90% (v/v) 1 M NaOH). Particles were imaged over time in these conditions. After 24 h, particle cores were fully degraded and microcapsules were formed. To prevent microcapsules from sticking to the glass slide and to aid in particle recovery, 25 μL of glycerol could be used to cover the glass bottom of the small well. Since the density of glycerol is slightly greater than that of the particles, this prevents the particles from coming into contact with the glass, which can sometimes lead to rupture of the capsule membrane. Microcapsules can be recovered by using a pipet to remove the particle solution from the well.

Fluorescence Microscopy. Epifluorescence images were obtained using an inverted microscope (Axio Observer.A1, Zeiss; 5×, 10×, and 20× objectives) connected to a cooled interline CCD camera (Clara, Andor). Confocal images were taken using a confocal laser scanning microscope (LSM 700, Zeiss; 20×, 40× oil, and 63× oil objectives).

Particle Tracking. Observation chambers were made as previously described.[30] 20 μL of a well-mixed solution containing 10% particles in PBST and 90% (v/v) 1 M NaOH was loaded into chambers made from a glass slide and a coverslip separated by two parallel strips of parafilm. The chamber was completely sealed using UV-cured optical glue (#65, Norland) to prevent drift and evaporation. Videos of 500−2500 frames were taken using an EB-CCD camera (C7190-43, Hamamatsu) connected to an inverted microscope (Axiovert 200, Zeiss) at a rate of 29.6 frames/s at room temperature. A public-domain MATLAB algorithm written by Kilfoil and co-workers[31] was used to identify fluorescent beads and track their two-dimensional trajectories (Figure S4). Trajectories were averaged to obtain the mean-squared displacement (MSD) as a function of lag time. Static error due to camera noise was determined by analyzing immobilized beads. Particle tracking accuracy was verified by analyzing videos of freely diffusing 200 nm polystyrene beads in water. The bulk diffusivity calculated from the MSD of beads in water matched the theoretical value (within 5% error).

EDC Coupling. Particles coated with PLL (10% v/v) were added to a solution of *N*-(3-(dimethylamino)propyl)-*N*′-ethylcarbodiimide hydrochloride (EDC) in PBST (final concentration 3 mg/mL). The mixture was placed on a horizontal shaker (750 rpm) at room temperature for 3.5 h. Particles were rinsed four times in PBST and stored in PBST at 4 °C.

RESULTS AND DISCUSSION

Polyelectrolyte Deposition on Hydrogel Templates. Figure 1 illustrates our general approach to create core−shell structures, selectively coat Janus particles, and synthesize microcapsules using SFL hydrogel templates. We first polymerize microparticles in the desired photomask-defined shapes (Figure 1A) using a prepolymer solution containing PEGDA, acrylic acid (AAc), and photoinitiator. The carboxylic groups from the AAc ($pK_a \sim 4.5$[32]) are covalently linked to the cross-linked PEG hydrogel, creating a negatively charged matrix at neutral pH. After collecting and washing the particles, we coat them with the biocompatible polycation, poly-L-lysine (PLL, M_v = 150−300 kDa), by immersing the particles in an aqueous solution of PLL with controlled pH and ionic strength. At neutral pH, the cationic PLL ($pK_a \sim 10.5$[33]) interacts with the

DOI: 10.1021/acs.langmuir.5b02200
Langmuir XXXX, XXX, XXX−XXX

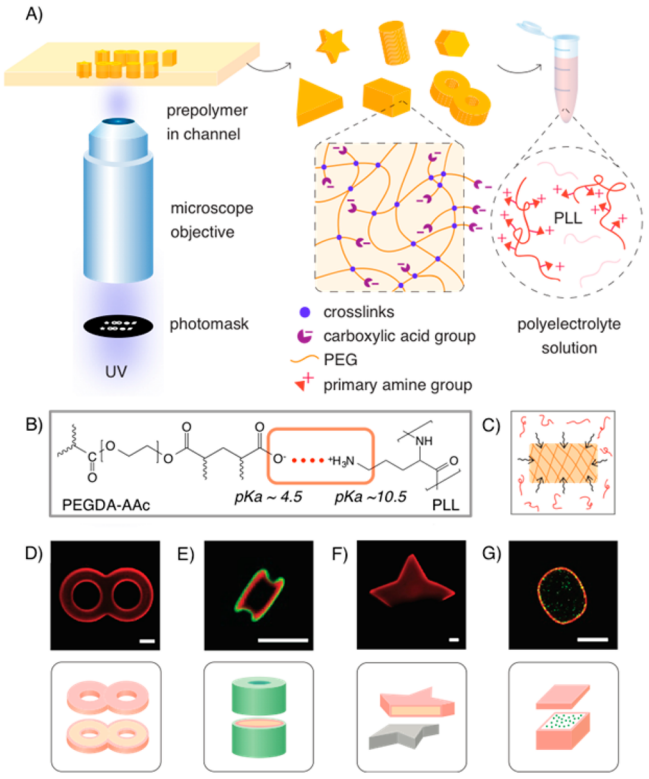

Figure 1. Synthesis of microcapsules using templates fabricated by stop flow lithography. A prepolymer solution consisting of poly(ethylene glycol) diacrylate (PEGDA) and acrylic acid (AAc) is polymerized within a microfluidic channel to form template hydrogel microparticles using SFL technique (A). The carboxylic acid groups within the hydrogel matrix are negatively charged at neutral pH, allowing uniform coating of the particle by the polycation poly-L-lysine (PLL) via electrostatic interactions (B, C). Excess polymer is washed away by centrifuging and additional layers of oppositely charged polymers can be added, or capsules can be made by dissolving away the sacrificial core using saponification at high pH (0.9 M NaOH). Fluorescence images show PLL coating on a genus-2 surface (D, confocal), two layer PLL (red)/dextran sulfate (green) coating (E, confocal), selective PLL coating of a Janus particle (F, epifluorescence), and a PLL capsule containing 200 nm polystyrene nanoparticles (G, confocal). Illustrations below fluorescence images show the particle interior and exterior. Scale bars are 30 μm.

anionic hydrogel particle via electrostatic interactions (Figure 1B). As a result, the PLL forms a uniform shell on the particle by diffusing into the outer edge of the hydrogel matrix (Figure 1C). We can then deposit additional layers of oppositely charged polyelectrolytes (e.g., dextran sulfate (DXS)) or dissolve away the template core to form hollow microcapsules. We show a sampling of particle morphologies achievable using this technique in Figure 1D–G. We demonstrate uniform PLL coating of a particle of topological genus 2 (shape with two holes) (Figure 1D), two-layer (PLL/DXS) coating of a three-dimensionally patterned shape fabricated by grayscale lithography[34] (Figure 1E), and selective coating of a Janus particle (Figure 1F). In Figure 1G, the template core has been removed to form a microcapsule encapsulating 200 nm fluorescent nanoparticles as model cargo.

This technique can be used for region-specific coating of Janus particles fabricated using two streams of prepolymer—one with acrylic acid and one without. As previously described,[8] Janus or multistripe particles can be easily fabricated by SFL using coflowing laminar streams in a multi-inlet microfluidic device. The PLL selectively coats the negatively charged portions of the particles, allowing for spatially controlled functionalization of hydrogel microparticles (Figure 2).

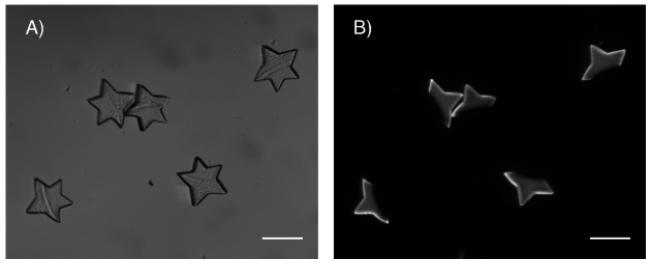

Figure 2. Selective coating of Janus particles. Bright field (A) and epifluorescence (B) images of Janus particles coated with one layer of Cy5-PLL. Janus star-shaped particles are made by coflowing two prepolymer streams—one with acrylic acid and one without. Only the portion of the particle that contains AAc, and is therefore negatively charged, is coated by PLL. This coating is only on the outer edge of the particles—the fluorescence of the inside is due to the coating on the exterior surface of the particles. A higher magnification fluorescence image is shown in Figure 1F. Scale bars are 200 μm.

In addition to partially coated Janus particles, we can form fully coated core–shell structures with shell thicknesses around 3–4 μm using a PLL solution with neutral pH and ionic strength between 0.5 and 1 M NaCl. We define shell thickness by the full width at half-maximum (fwhm) extracted from fluorescence intensity profiles of confocal images of Cy5-PLL coated particles. Shells are formed by diffusion of the PLL into the hydrogel matrix, which differs from conventional nanometer scale LbL layers that are built on top of nonporous substrates.[35,36] The extent of diffusion of PLL into the matrix depends on a combination of steric and electrostatic effects.[37]

We observed the contribution of steric effects by altering PLL molecular weight and PEGDA concentration. At pH 7/0.5 M NaCl, $PLL_{15-30\,kDa}$ diffuses into the entire hydrogel, while $PLL_{150-300\,kDa}$ (used in the majority of this work) forms a shell (Figure S1), similar to what is observed by Bysell and coworkers in a PLL/poly(acrylic acid) microgel system.[38] Also as expected, increasing PEGDA concentration decreases the mesh size of the gel[39] and consequently decreases the thickness of the shell by limiting the diffusion of PLL into the hydrogel[40] (Figure 3D, at constant pH of 7 and ionic strength of 0.5 M NaCl).

As shown in Figure 3A,B, increasing the ionic strength from 0 to 1 M NaCl (pH held constant at 7) decreases the extent of PLL diffusion into the particle, creating thinner and more well-defined shells. These thin shells are believed to result from two physical processes. First, there is a reduction in the hydrogel mesh size due to decreased swelling of the PEGDA-AAc particle (Figure S2) by the Donnan effect.[37,41] Second, the charge screening at higher ionic strength enables denser packing of PLL molecules in the outer region of the particle, which sterically prevents further inward diffusion of other PLL molecules. A similar trend was observed by Kaufman et al. during the fabrication of polyelectrolyte microcapsules across water/oil droplet interfaces.[42] As expected, polyelectrolyte deposition at extremely high ionic strength (i.e., 5 M NaCl) is unsuccessful due to complete charge screening.

At very low or very high pH (<2 or >12), the hydrogel or PLL is respectively no longer charged, and no PLL is deposited

DOI: 10.1021/acs.langmuir.5b02200
Langmuir XXXX, XXX, XXX–XXX

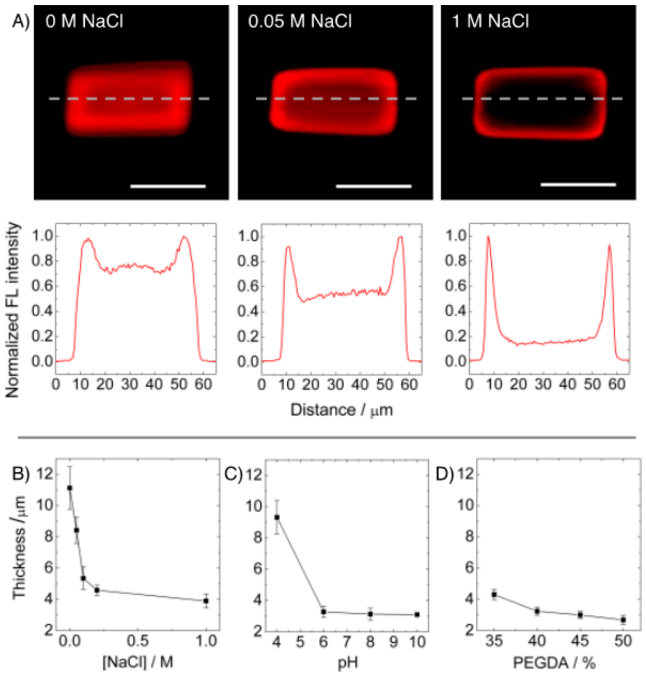

Figure 3. Controlling the diffusion of PLL into hydrogel templates. Confocal micrographs and fluorescence intensity profiles across the indicated cross sections show the diffusion of Cy5-PLL (MW: 150–300 kDa) into PEGDA-AAc hydrogel particles for different ionic strengths (A). The extent of diffusion of PLL into the particle is determined by steric effects and the strength of the electrostatic interaction between PEGDA-AAc and PLL. Shell thicknesses, defined as the fwhm extracted from fluorescence intensity profiles, are plotted as a function of the ionic strength of the PLL deposition solution (B; pH = 7, PEGDA = 50%), the pH of the PLL solution (C; [NaCl] = 0.5M, PEGDA = 50%), and the PEGDA concentration (v/v) of the prepolymer solution (D; pH = 7, [NaCl] = 0.5 M), N = 10 (error bars represent standard deviation). Scale bars are 30 μm.

in either case. At a pH close to the pK_a of the hydrogel matrix (ionic strength held constant at 0.5 M NaCl), the PLL completely diffuses into the particle, while at a pH range where both the PLL and the PEGDA-AAc are charged, a thin shell forms (Figure 3C). This suggests that inward diffusion is impeded by an increase in charge density of one of the interacting species. High charge density of PLL or PEGDA-AAc results in immediate complexation of the two species that prevents further inward diffusion of PLL, while the longer reaction time scale for less densely charged species allows PLL to penetrate further into the hydrogel matrix. Changing the time of PLL incubation from 1 min to 1 h results in no significant difference in shell thicknesses, indicating that both reaction and diffusion occur on time scales less than 1 min.

By studying the effects of pH, ionic strength, and prepolymer PEGDA concentration on PLL diffusion, we demonstrate how to control polyelectrolyte deposition onto hydrogel templates. In this study, the parameters we chose were suitable for creating micron thick shells on microparticles with dimensions greater than 10 μm. However, for applications such as drug delivery, smaller particles and capsules are more desirable. Our group has recently shown that it is possible to make colloidal particles with dimensions from 1 to 10 μm using oxygen-controlled SFL.[30] It should be possible to create thinner shells on these smaller particles by finding suitable materials and deposition parameters—for example, Wong et al. showed polyelectrolyte diffusion into soft, porous hydrogel substrates with estimated layer thicknesses on the nanometer scale.[43] Optimization of parameters will allow for fabrication of PLL shells on SFL particles of various sizes, which can then be easily converted into microcapsules.

Degradation of Hydrogel Templates to Form Microcapsules. To make hollow microcapsules, we simply immerse hydrogel particles with a single-layer PLL shell in basic conditions (0.9 M NaOH) to degrade the particle core via ester hydrolysis (Figure 4). While uncoated particles

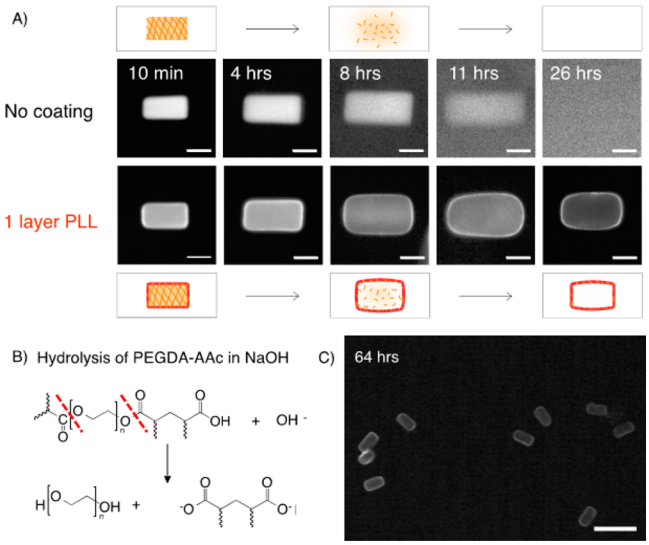

Figure 4. Degradation of hydrogel templates to form PLL capsules. Uncoated and Cy5-PLL (MW: 150–300 kDa) coated hydrogel particles are immersed in 0.9 M NaOH and monitored with fluorescence microscopy over time (rhodamine acrylate dye is copolymerized into the hydrogel) (A, scale bars are 30 μm). Degradation of the PEGDA-AAc core is due to base-catalyzed hydrolysis of ester bonds in the hydrogel (B). Low-magnification fluorescent image shows intact PLL capsules after 64 h incubation in NaOH (C, scale bar is 200 μm).

completely disintegrate under these conditions, PLL shells remain intact (Figure 4A). The particles swell during the hydrolysis process due to osmotic pressure caused by the breakup of the cross-linked polymer into smaller fragments (Figure 4B). After 26 h, the capsules begin to revert back toward their initial size and shape when fully cleaved degradation products are able to diffuse through the remaining membrane, causing osmotic pressure to decrease. Quantification of capsule dimensions during the degradation process shows that capsules eventually return to their photomask-defined sizes, demonstrating the precise control over capsule shape and size achievable using this technique (Table S1). The capsules remain intact for more than 2 weeks in hydrolytic conditions (pH 14).

To quantify the degradation process, we performed particle tracking on hydrogel microparticles synthesized with embedded 200 nm diameter carboxylate polystyrene beads. Particle tracking is commonly used to interrogate the evolving mechanical properties of cells using beads embedded in the cell cytoplasm.[44] More recently, particle tracking has been used to monitor hydrogel degradation via metalloproteinases.[45] In our study, the beads were physically trapped in the polymerized PEGDA-AAc hydrogel particle, initially static due to the tight

DOI: 10.1021/acs.langmuir.5b02200
Langmuir XXXX, XXX, XXX−XXX

mesh of the intact hydrogel. As the hydrogel is degraded in NaOH, the gel porosity increases and the beads begin to move (Figure 5A). The plot of the beads' mean-square displacement

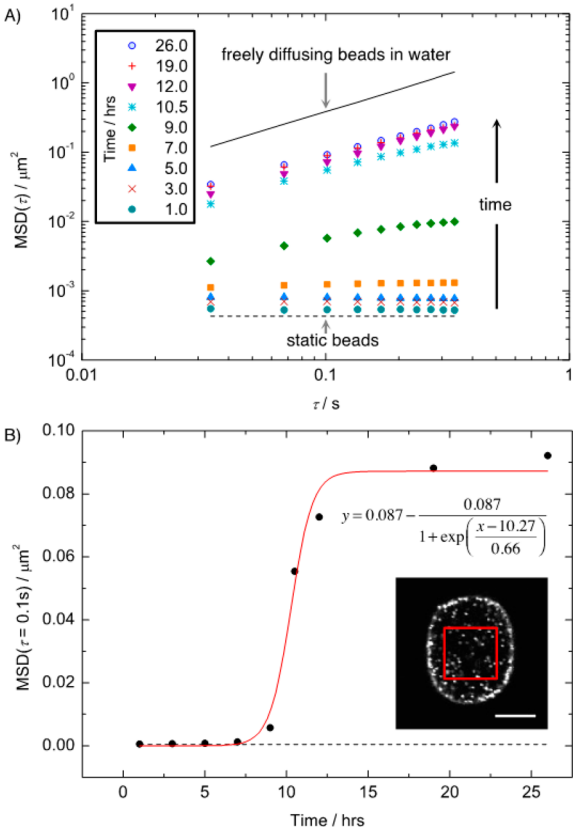

Figure 5. Quantifying hydrogel degradation over time using particle tracking. 200 nm diameter YG carboxylate polystyrene beads embedded into hydrogel particles are monitored by particle tracking after immersing Cy5-PLL-coated particles in 0.9 M NaOH. Mean-squared displacements (MSDs) of beads in the center of hydrogel particles (inset) are plotted as a function of lag time (τ) for various time points in the core degradation process. MSDs in bulk for freely diffusing beads in water are plotted for comparison (A). MSDs at τ = 0.1 s are plotted with respect to time immersed in NaOH (the red curve is a fit to the data, described by the given equation) (B). The dashed line on both plots represents the MSD for immobilized beads due to static noise.[48] Scale bar for inset is 20 μm.

(MSD at lag time = 0.1s) over time shows that bead motion increases suddenly after ~10 h incubation in 0.9 M NaOH, suggesting a characteristic time scale for the bulk degradation of the hydrogel (Figure 5B). The slight plateau of MSDs at longer time lags for intermediate time points (Figure 5A, 9–12 h curves) suggests that beads are locally confined, representing typical behavior for a gel.[46,47] After a period of 19 h, there is no longer any significant change in the MSDs. We tracked freely diffusing beads in water to obtain an upper bound representing purely diffusive behavior and used immobilized beads to obtain the static error due to camera noise.[48] From these particle tracking measurements, we conclude that the hydrogel core has been fully degraded after 19 h, allowing for diffusion of embedded beads. However, we observe that the final MSD of diffusing beads within the particles at long time points is less than that of freely diffusing beads in water. This is likely due to the presence of higher viscosity PEGDA monomer within the observation chamber solution, from degradation of the core. Particle tracking videos at long time points also show that only beads in the center of the microcapsules diffuse and that beads embedded within the PLL shell remain static. The diffusing beads remain confined within intact microcapsules for more than 2 weeks (see Video S1).

The fluorescent polystyrene nanoparticles represent model cargo that can be encapsulated within SFL-templated microcapsules. It should also be possible to encapsulate smaller cargo, down to tens of nanometers in size, by tuning the pore size of the capsule membrane. This may be achievable through denser packing of PLL controlled by deposition conditions, by adjusting the molecular weight of both the PEGDA and the PLL, or by adding additional coating layers. Changing the permeability of the capsule membrane may add additional functionality for encapsulation and controlled release of different compounds. Capsules have been observed to release their contents when exterior stress causes the membrane to rupture. Possible reasons for membrane rupture include adhesion to glass slides or other capsules, osmotic shock due to changing ionic strength of the surrounding solution, or mechanical forces that cause extreme capsule deformation. Our results suggest that microcapsules can be used as containers to encapsulate various types of cargo that can be embedded within the hydrogel template and that this cargo can remain trapped until the capsule disintegrates or ruptures. Although our current technique uses harsh conditions for template core removal, we can alter our hydrogel chemistry to allow for mild degradation conditions suitable for encapsulation of biologically relevant cargo. For example, we can fabricate hydrogel templates using a diacrylated poly(lactic acid)–PEG block copolymer that has been shown to degrade in physiological conditions after 1 week, as demonstrated in previous work from our group.[49]

Since microcapsules retain the complex shapes of their lithographically defined templates, we are able to make novel capsule shapes that cannot be easily fabricated with any other technique. For example, Figure 6 shows genus 1 and 2 microcapsules, similar to shapes observed in phospholipid

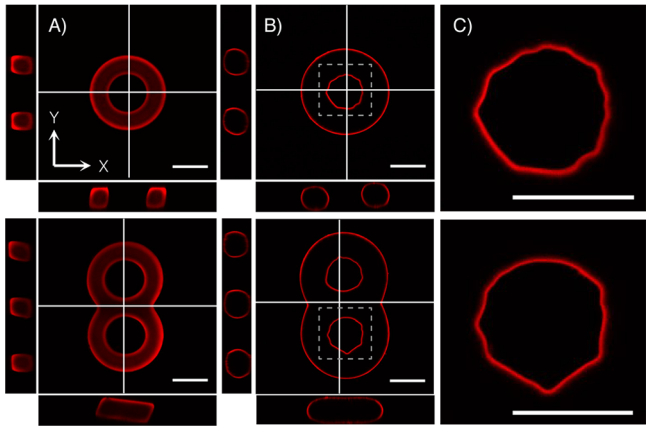

Figure 6. Microcapsules made from templates with internal features. Genus 1 and 2 particles are coated with Cy5-PLL, and the template cores are subsequently dissolved in 0.9 M NaOH to form capsules. Particles are imaged by confocal fluorescence microscopy before (A) and during core dissolution after 19 h in 0.9 M NaOH (B). Swelling in NaOH due to osmotic pressure causes stretching of the outer membrane and buckling of the inner membrane. A close-up shows detail of the buckled inner membrane (C). Cross-sectional views (*YZ* and *XZ*) are shown for the slices indicated by the white lines in the *XY* view. Scale bars are 50 μm.

DOI: 10.1021/acs.langmuir.5b02200
Langmuir XXXX, XXX, XXX–XXX

vesicles.[50] The genus 2 capsule is a double-holed torus. Confocal images of swollen microcapsules show that osmotic pressure in these genus 1+ capsules leads to expansion of the outer membrane and buckling of the inner membrane (Figure 6B,C). This enables future studies of mechanical properties of thin polymer membranes.[51,52]

The deformation of capsule membranes in response to osmotic stress is one demonstration of the flexible nature of these hollow microcapsules. To further test their deformability, we collected microcapsules after complete core removal (9 days in 0.9 M NaOH) and loaded them into a microfluidic channel with a contraction (channel height: 60 μm, wide section: 300 μm wide × 3300 μm long, contraction: 30 μm wide × 300 μm long). Figure 7 shows a representative example of a rectangular

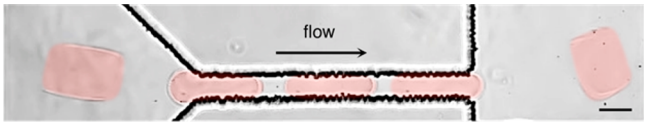

Figure 7. Microcapsules deform and recover shape. Composite image of frames from a video (30 fps, Nikon D7000, see Video S2) showing a capsule (after 9 days in 0.9 M NaOH) flowing through a microfluidic contraction. Motion is from left to right (t_1 = 0, t_2 = 33 ms, t_3 = 200 ms, t_4 = 266 ms, t_5 = 300 ms). Flow is driven by a small hydrostatic pressure, and flow rate is less than 10 μL/min. The image has been false colored to accentuate the capsule. Scale bar is 50 μm.

microcapsule (63 μm wide × 89 μm long, 58 μm in height) deforming to pass through the contraction under manually applied pressure and recovering its original shape on the other side of the contraction. We believe that these flexible capsules have potential to make good model systems for studying nonspherical capsule flow dynamics.[53]

After observing the stability and mechanical flexibility of these microcapsules, we sought to determine the mechanism for how these capsules remain intact under harsh basic conditions. Since the hydrogel templates are coated by PLL via electrostatic interactions, we anticipated that the majority of neutral PLL would dissociate from the PEGDA-AAc core at pH 14. We tested this by observing the change in fluorescence intensity of PLL coated particles upon immersion in 0.9 M NaOH. As a positive control, we covalently linked the PLL to the hydrogel matrix by forming stable amide bonds using carbodiimide (EDC) chemistry.[54] Amide-based hydrogels are stable under conditions that hydrolyze ester-based gels.[55,56] Figure 8 compares the fluorescence intensity for particles in PBS and 5 min after immersion in 0.9 M NaOH, under identical imaging conditions. Note that in the bottom left image of Figure 8 (no EDC, pH 14) the particle is present but undetectable when the fluorescence intensity is normalized. This provides evidence that a significant portion of PLL does immediately dissociate in highly alkaline conditions when it is not covalently linked to the PEGDA-AAc hydrogel. However, we suspect that a very small amount of PLL remains and forms amide linkages to the PEGDA-AAc, which is expected under basic conditions.[57] By covalently linking to the PEGDA-AAc, the PLL acts to cross-link the shell, preventing degradation of the hydrogel matrix where PLL is present. This hypothesis is consistent with FTIR analysis of bulk samples before and after degradation for plain PEGDA-AAc, PEGDA-AAc with PLL, and PEGDA-AAC with PLL cross-linked with EDC (Figure S4). To achieve similar results, other groups have covalently

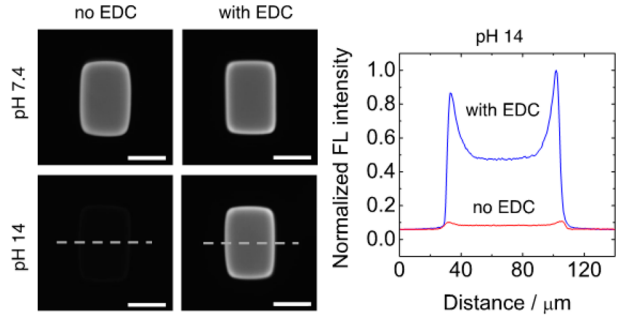

Figure 8. EDC coupling prevents immediate dissociation of Cy5-PLL in 0.9 M NaOH. A comparison between Cy5-PLL coated particles with and without EDC cross-linking in PBS (pH 7.4) and after 5 min in 0.9 M NaOH (pH 14). The fluorescence intensity dramatically decreases after immersion in NaOH for particles without EDC coupling but remains the same for PLL-coated particles with EDC coupling. All particles are imaged by epifluorescence with the same imaging conditions and displayed with intensities normalized across all four images. The fluorescence intensity profiles for the indicated cross sections of particles in NaOH are plotted on the right (normalized to the maximum intensity of the EDC particle). Scale bars are 50 μm.

linked polyelectrolyte multilayers through amide bonds using heat,[58] polyelectrolytes with chemically reactive end groups,[59] or EDC chemistry.[60] One advantage of our current technique is the single-step simultaneous core removal and shell cross-linking procedure. Since the edges of the hydrogel template are cross-linked by the PLL to form a stable shell, a small amount of template material remains in the capsule. This is confirmed in particle tracking videos showing static beads trapped in the shell (Video S1). However, in contrast to conventional LbL capsules where complete template removal is desirable due to template incompatibility with biological systems, our PEGDA hydrogel templates are biocompatible, and remnants of the material within the shell do not limit the capsules' use in potential applications. This remnant material could also be beneficial in some applications. For example, it can be readily functionalized with DNA and antibodies or serve to control the porosity and/or modulus of the capsule.

CONCLUSIONS

We have demonstrated how hydrogel microparticles fabricated by SFL can be used as templates to create custom shape microcapsules via a simple and controllable polyelectrolyte deposition and core dissolution process. The unique advantages of this approach include the ability to create flexible microcapsules that retain complex (e.g., genus 1+) template geometries and the ability to selectively functionalize the surface of Janus particles. In addition, we believe that our technique can be easily modified to use mild processing conditions suitable for encapsulation of biologically active compounds. Future studies will focus on interrogating the mechanical properties of these capsules as well as investigating the controlled release of encapsulated compounds of interest. This will allow future development of these designer microcapsules for use in drug delivery, in tissue engineering, or as model systems for studying their flow dynamics or membrane mechanics.

DOI: 10.1021/acs.langmuir.5b02200
Langmuir XXXX, XXX, XXX−XXX

■ ASSOCIATED CONTENT

Supporting Information

The Supporting Information is available free of charge on the ACS Publications website at DOI: 10.1021/acs.langmuir.5b02200.

Figures showing (i) effect of PLL molecular weight on coating, (ii) swelling of PEGDA-AAc particles, (iii) particle tracking images, and (iv) FTIR spectra of bulk samples; table showing particle dimensions during and after template removal (PDF)

Movie showing microcapsules with encapsulated nanoparticles (AVI)

Movie showing capsule flow through a contraction (AVI)

■ AUTHOR INFORMATION

Corresponding Author

*E-mail pdoyle@mit.edu (P.S.D.).

Notes

The authors declare no competing financial interest.

■ ACKNOWLEDGMENTS

This work is supported by the Institute for Collaborative Biotechnologies through grant W911NF-09-0001 from the U.S. Army Research Office. The content of the information does not necessarily reflect the position or the policy of the Government, and no official endorsement should be inferred. Additional support was provided by NSF grants CMMI-1120724 and DMR-1006147. We thank Octavio Hurtado for help with device microfabrication at the BioMEMS Resource Center, Wendy Salmon for confocal microscopy training, Stephen Morton for helpful discussions, and Nima Yazdan Panah and Tim McClure for FTIR assistance. L.C. is supported in part by a postgraduate scholarship from Natural Sciences and Engineering Research Council (NSERC) of Canada.

■ REFERENCES

(1) Venkataraman, S.; Hedrick, J. L.; Ong, Z. Y.; Yang, C.; Ee, P. L. R.; Hammond, P. T.; Yang, Y. Y. The Effects of Polymeric Nanostructure Shape on Drug Delivery. *Adv. Drug Delivery Rev.* **2011**, *63* (14−15), 1228−1246.

(2) Yoo, J.-W.; Irvine, D. J.; Discher, D. E.; Mitragotri, S. Bio-Inspired, Bioengineered and Biomimetic Drug Delivery Carriers. *Nat. Rev. Drug Discovery* **2011**, *10* (7), 521−535.

(3) Mitragotri, S.; Lahann, J. Physical Approaches to Biomaterial Design. *Nat. Mater.* **2009**, *8* (1), 15−23.

(4) Shimoni, O.; Yan, Y.; Wang, Y.; Caruso, F. Shape-Dependent Cellular Processing of Polyelectrolyte Capsules. *ACS Nano* **2013**, *7* (1), 522−530.

(5) Best, J. P.; Yan, Y.; Caruso, F. The Role of Particle Geometry and Mechanics in the Biological Domain. *Adv. Healthcare Mater.* **2012**, *1* (1), 35−47.

(6) Glotzer, S. C.; Solomon, M. J. Anisotropy of Building Blocks and Their Assembly into Complex Structures. *Nat. Mater.* **2007**, *6* (8), 557−562.

(7) Dendukuri, D.; Doyle, P. S. The Synthesis and Assembly of Polymeric Microparticles Using Microfluidics. *Adv. Mater.* **2009**, *21* (41), 4071−4086.

(8) Dendukuri, D.; Pregibon, D. C.; Collins, J.; Hatton, T. A.; Doyle, P. S. Continuous-Flow Lithography for High-Throughput Microparticle Synthesis. *Nat. Mater.* **2006**, *5* (5), 365−369.

(9) Rolland, J.; Maynor, B.; Euliss, L.; Exner, A.; Denison, G.; DeSimone, J. Direct Fabrication and Harvesting of Monodisperse, Shape-Specific Nanobiomaterials. *J. Am. Chem. Soc.* **2005**, *127*, 10096−10100.

(10) Roh, K.; Martin, D. C.; Lahann, J. Biphasic Janus Particles with Nanoscale Anisotropy. *Nat. Mater.* **2005**, *4* (10), 759−763.

(11) Shum, H. C.; Abate, A. R.; Lee, D.; Studart, A. R.; Wang, B.; Chen, C.-H.; Thiele, J.; Shah, R. K.; Krummel, A.; Weitz, D. A. Droplet Microfluidics for Fabrication of Non-Spherical Particles. *Macromol. Rapid Commun.* **2010**, *31* (2), 108−118.

(12) Champion, J. A.; Katare, Y. K.; Mitragotri, S. Making Polymeric Micro- and Nanoparticles of Complex Shapes. *Proc. Natl. Acad. Sci. U. S. A.* **2007**, *104* (29), 11901−11904.

(13) Morton, S. W.; Herlihy, K. P.; Shopsowitz, K. E.; Deng, Z. J.; Chu, K. S.; Bowerman, C. J.; Desimone, J. M.; Hammond, P. T. Scalable Manufacture of Built-to-Order Nanomedicine: Spray-Assisted Layer-by-Layer Functionalization of PRINT Nanoparticles. *Adv. Mater.* **2013**, *25* (34), 4707−4713.

(14) Doshi, N.; Zahr, A. S.; Bhaskar, S.; Lahann, J.; Mitragotri, S. Red Blood Cell-Mimicking Synthetic Biomaterial Particles. *Proc. Natl. Acad. Sci. U. S. A.* **2009**, *106* (51), 21495−21499.

(15) Zan, X.; Garapaty, A.; Champion, J. A. Engineering Polyelectrolyte Capsules with Independently Controlled Size and Shape. *Langmuir* **2015**, *31* (27), 7601−7608.

(16) Shaillender, M.; Luo, R.; Venkatraman, S. S.; Neu, B. Layer-by-Layer Microcapsules Templated on Erythrocyte Ghost Carriers. *Int. J. Pharm.* **2011**, *415* (1−2), 211−217.

(17) Donath, E.; Moya, S.; Neu, B.; Sukhorukov, G. B.; Radostina, G.; Voigt, A.; Baumler, H.; Kiesewetter, H.; Mohwald, H. Hollow Polymer Shells from Biological Templates: Fabrication. *Chem. - Eur. J.* **2002**, *8* (23), 5481−5485.

(18) Yashchenok, A.; Parakhonskiy, B.; Donatan, S.; Kohler, D.; Skirtach, A.; Möhwald, H. Polyelectrolyte Multilayer Microcapsules Templated on Spherical, Elliptical and Square Calcium Carbonate Particles. *J. Mater. Chem. B* **2013**, *1* (9), 1223.

(19) Shchepelina, O.; Lisunova, M. O.; Drachuk, I.; Tsukruk, V. V. Morphology and Properties of Microcapsules with Different Core Releases. *Chem. Mater.* **2012**, *24* (7), 1245−1254.

(20) Kozlovskaya, V.; Alexander, J. F.; Wang, Y.; Kuncewicz, T.; Liu, X.; Godin, B.; Kharlampieva, E. Internalization of Red Blood Cell-Mimicking Hydrogel Capsules with pH-Triggered Shape Responses. *ACS Nano* **2014**, *8* (6), 5725−5737.

(21) Rozynek, Z.; Mikkelsen, A.; Dommersnes, P.; Fossum, J. O. Electroformation of Janus and Patchy Capsules. *Nat. Commun.* **2014**, *5*, 3945.

(22) Studart, A. R.; Shum, H. C.; Weitz, D. A. Arrested Coalescence of Particle-Coated Droplets into Nonspherical Supracolloidal Structures. *J. Phys. Chem. B* **2009**, *113* (12), 3914−3919.

(23) Pawar, A. B.; Caggioni, M.; Ergun, R.; Hartel, R. W.; Spicer, P. T. Arrested Coalescence in Pickering Emulsions. *Soft Matter* **2011**, *7* (17), 7710.

(24) Subramaniam, A. B.; Abkarian, M.; Mahadevan, L.; Stone, H. A. Colloid Science: Non-Spherical Bubbles. *Nature* **2005**, *438* (7070), 930.

(25) Datta, S. S.; Abbaspourrad, A.; Amstad, E.; Fan, J.; Kim, S.-H.; Romanowsky, M.; Shum, H. C.; Sun, B.; Utada, A. S.; Windbergs, M.; et al. 25th Anniversary Article: Double Emulsion Templated Solid Microcapsules: Mechanics And Controlled Release. *Adv. Mater.* **2014**, *26* (14), 2205−2218.

(26) Dendukuri, D.; Gu, S. S.; Pregibon, D. C.; Hatton, T. A.; Doyle, P. S. Stop-Flow Lithography in a Microfluidic Device. *Lab Chip* **2007**, *7* (7), 818−828.

(27) An, H. Z.; Helgeson, M. E.; Doyle, P. S. Nanoemulsion Composite Microgels for Orthogonal Encapsulation and Release. *Adv. Mater.* **2012**, *24* (28), 3838−3844 3895..

(28) An, H. Z.; Safai, E. R.; Burak Eral, H.; Doyle, P. S. Synthesis of Biomimetic Oxygen-Carrying Compartmentalized Microparticles Using Flow Lithography. *Lab Chip* **2013**, *13* (24), 4765−4774.

(29) Appleyard, D. C.; Chapin, S. C.; Srinivas, R. L.; Doyle, P. S. Bar-Coded Hydrogel Microparticles for Protein Detection: Synthesis, Assay and Scanning. *Nat. Protoc.* **2011**, *6* (11), 1761−1774.

DOI: 10.1021/acs.langmuir.5b02200
Langmuir XXXX, XXX, XXX−XXX

(30) An, H. Z.; Eral, H. B.; Chen, L.; Chen, M. B.; Doyle, P. S. Synthesis of Colloidal Microgels Using Oxygen-Controlled Flow Lithography. *Soft Matter* **2014**, *10*, 7595−7605.
(31) Pelletier, V.; Gal, N.; Fournier, P.; Kilfoil, M. L. Microrheology of Microtubule Solutions and Actin-Microtubule Composite Networks. *Phys. Rev. Lett.* **2009**, *102* (18), 100−103.
(32) Jabbari, E.; Nozari, S. Swelling Behavior of Acrylic Acid Hydrogels Prepared by c-Radiation Crosslinking of Polyacrylic Acid in Aqueous Solution. *Eur. Polym. J.* **2000**, *36*, 2685−2692.
(33) Mirtič, A.; Grdadolnik, J. The Structure of Poly-L-Lysine in Different Solvents. *Biophys. Chem.* **2013**, *175*−*176*, 47−53.
(34) Galas, J. C.; Belier, B.; Aassime, A.; Palomo, J.; Bouville, D.; Aubert, J. Fabrication of Three-Dimensional Microstructures Using Standard Ultraviolet and Electron-Beam Lithography. *J. Vac. Sci. Technol., B: Microelectron. Process. Phenom.* **2004**, *22* (3), 1160.
(35) Li, Y.; Wang, X.; Sun, J. Layer-by-Layer Assembly for Rapid Fabrication of Thick Polymeric Films. *Chem. Soc. Rev.* **2012**, *41* (18), 5998−6009.
(36) Shiratori, S. S.; Rubner, M. F. pH-Dependent Thickness Behavior of Sequentially Adsorbed Layers of Weak Polyelectrolytes. *Macromolecules* **2000**, *33* (11), 4213−4219.
(37) Horvath, A. T.; Horvath, A. E.; Lindstrom, T.; Wågberg, L. Diffusion of Cationic Polyelectrolytes into Cellulosic Fibers. *Langmuir* **2008**, *24*, 10797−10806.
(38) Bysell, H.; Hansson, P.; Malmsten, M. Transport of Poly-L-Lysine into Oppositely Charged Poly(acrylic Acid) Microgels and Its Effect on Gel Deswelling. *J. Colloid Interface Sci.* **2008**, *323* (1), 60−69.
(39) Waters, D. J.; Engberg, K.; Parke-Houben, R.; Hartmann, L.; Ta, C. N.; Toney, M. F.; Frank, C. W. Morphology of Photopolymerized End-Linked Poly(ethylene Glycol) Hydrogels by Small-Angle X-Ray Scattering. *Macromolecules* **2010**, *43* (16), 6861−6870.
(40) Jianhao, B.; Sebastian, B.; Yein, T. S.; Dieter, T. Self-Assembly of Polyamines as a Facile Approach to Fabricate Permeability Tunable Polymeric Shells for Biomolecular Encapsulation. *ACS Appl. Mater. Interfaces* **2011**, *3*, 1665−1674.
(41) Smith, M. H.; Lyon, L. A. Tunable Encapsulation of Proteins within Charged Microgels. *Macromolecules* **2011**, *44*, 8154−8160.
(42) Kaufman, G.; Boltyanskiy, R.; Nejati, S.; Thiam, A.; Loewenberg, M.; Dufresne, E.; Osuji, C. Single-Step Microfluidic Fabrication of Soft Monodisperse Polyelectrolyte Microcapsules by Interfacial Complexation. *Lab Chip* **2014**, *14*, 3494−3497.
(43) Wong, J. E.; Diez-Pascual, A. M.; Richtering, W. Layer-by-Layer Assembly of Polyelectrolyte Multilayers on Thermoresponsive P (NiPAM- Co -MAA) Microgel. *Macromolecules* **2009**, *42*, 1229−1238.
(44) Wirtz, D. Particle-Tracking Microrheology of Living Cells: Principles and Applications. *Annu. Rev. Biophys.* **2009**, *38*, 301−326.
(45) Schultz, K. M.; Anseth, K. S. Monitoring Degradation of Matrix Metalloproteinases-Cleavable PEG Hydrogels via Multiple Particle Tracking Microrheology. *Soft Matter* **2013**, *9* (5), 1570.
(46) Valentine, M. T.; Perlman, Z. E.; Gardel, M. L.; Shin, J. H.; Matsudaira, P.; Mitchison, T. J.; Weitz, D. A. Colloid Surface Chemistry Critically Affects Multiple Particle Tracking Measurements of Biomaterials. *Biophys. J.* **2004**, *86* (6), 4004−4014.
(47) Petka, W. A.; Harden, J. L.; McGrath, K. P.; Wirtz, D.; Tirrell, D. A. Reversible Hydrogels from Self-Assembling Artificial Proteins. *Science* **1998**, *281* (5375), 389−392.
(48) Savin, T.; Doyle, P. S. Static and Dynamic Errors in Particle Tracking Microrheology. *Biophys. J.* **2005**, *88* (1), 623−638.
(49) Hwang, D. K.; Oakey, J.; Toner, M.; Arthur, J. A.; Anseth, K. S.; Lee, S.; Zeiger, A.; Van Vliet, K. J.; Doyle, P. S. Stop-Flow Lithography for the Production of Shape-Evolving Degradable Microgel Particles. *J. Am. Chem. Soc.* **2009**, *131* (12), 4499−4504.
(50) Michalet, X.; Bensimon, D. Observation of Stable Shapes and Conformal Diffusion in Genus 2 Vesicles. *Science* **1995**, *269* (5224), 666−668.
(51) Vliegenthart, G. A.; Gompper, G. Compression, Crumpling and Collapse of Spherical Shells and Capsules. *New J. Phys.* **2011**, *13*, 045020.
(52) Gao, C.; Donath, E.; Moya, S.; Dudnik, V.; Möhwald, H. Elasticity of Hollow Polyelectrolyte Capsules Prepared by the Layer-by-Layer Technique. *Eur. Phys. J. E: Soft Matter Biol. Phys.* **2001**, *5* (1), 21−27.
(53) Lefebvre, Y.; Leclerc, E.; Barthès-Biesel, D.; Walter, J.; Edwards-Lèvy, F. Flow of Artificial Microcapsules in Microfluidic Channels: A Method for Determining the Elastic Properties of the Membrane. *Phys. Fluids* **2008**, *20* (12), 123102.
(54) Nakajima, N.; Ikada, Y. Mechanism of Amide Formation by Carbodiimide for Bioconjugation in Aqueous Media. *Bioconjugate Chem.* **1995**, *6* (1), 123−130.
(55) Elbert, D. L.; Hubbell, J. A. Conjugate Addition Reactions Combined with Free-Radical Cross-Linking for the Design of Materials for Tissue Engineering. *Biomacromolecules* **2001**, *2* (2), 430−441.
(56) Browning, M. B.; Cosgriff-Hernandez, E. Development of a Biostable Replacement for PEGDA Hydrogels. *Biomacromolecules* **2012**, *13* (3), 779−786.
(57) Carey, F. A. *Organic Chemistry*, 4th ed.; McGraw-Hill Higher Education: Boston, MA, 2000.
(58) Harris, J. J.; DeRose, P. M.; Bruening, M. L. Synthesis of Passivating, Nylon-like Coatings through Cross-Linking of Ultrathin Polyelectrolyte Films [13]. *J. Am. Chem. Soc.* **1999**, *121* (9), 1978−1979.
(59) Gardner, C. M.; Burke, N. A. D.; Stöver, H. D. H. Cross-Linked Microcapsules Formed from Self-Deactivating Reactive Polyelectrolytes. *Langmuir* **2010**, *26* (7), 4916−4924.
(60) Lee, H.; Jeong, Y.; Park, T. G. Shell Cross-Linked Hyaluronic Acid/polylysine Layer-by-Layer Polyelectrolyte Microcapsules Prepared by Removal of Reducible Hyaluronic Acid Microgel Cores. *Biomacromolecules* **2007**, *8* (12), 3705−3711.

DOI: 10.1021/acs.langmuir.5b02200
Langmuir XXXX, XXX, XXX−XXX